

Net Charge Fluctuations in Au + Au Interactions at $\sqrt{s_{NN}} = 130$ GeV

K. Adcox,⁴⁰ S. S. Adler,³ N. N. Ajitanand,²⁷ Y. Akiba,¹⁴ J. Alexander,²⁷ L. Aphecetche,³⁴ Y. Arai,¹⁴ S. H. Aronson,³ R. Averbeck,²⁸ T. C. Awes,²⁹ K. N. Barish,⁵ P. D. Barnes,¹⁹ J. Barrette,²¹ B. Bassalleck,²⁵ S. Bathe,²² V. Baublis,³⁰ A. Bazilevsky,^{12,32} S. Belikov,^{12,13} F. G. Bellaiche,²⁹ S. T. Belyaev,¹⁶ M. J. Bennett,¹⁹ Y. Berdnikov,³⁵ S. Botelho,³³ M. L. Brooks,¹⁹ D. S. Brown,²⁶ N. Bruner,²⁵ D. Bucher,²² H. Buesching,²² V. Bumazhnov,¹² G. Bunce,^{3,32} J. Burward-Hoy,²⁸ S. Butsyk,^{28,30} T. A. Carey,¹⁹ P. Chand,² J. Chang,⁵ W. C. Chang,¹ L. L. Chavez,²⁵ S. Chernichenko,¹² C. Y. Chi,⁸ J. Chiba,¹⁴ M. Chiu,⁸ R. K. Choudhury,² T. Christ,²⁸ T. Chujo,^{3,39} M. S. Chung,^{15,19} P. Chung,²⁷ V. Cianciolo,²⁹ B. A. Cole,⁸ D. G. D'Enterria,³⁴ G. David,³ H. Delagrangé,³⁴ A. Denisov,¹² A. Deshpande,³² E. J. Desmond,³ O. Dietzsch,³³ B. V. Dinesh,² A. Drees,²⁸ A. Durum,¹² D. Dutta,² K. Ebisu,²⁴ Y. V. Efremenko,²⁹ K. El Chenawi,⁴⁰ H. En'yo,^{17,31} S. Esumi,³⁹ L. Ewell,³ T. Ferdousi,⁵ D. E. Fields,²⁵ S. L. Fokin,¹⁶ Z. Fraenkel,⁴² A. Franz,³ A. D. Frawley,⁹ S.-Y. Fung,⁵ S. Garpman,^{20,*} T. K. Ghosh,⁴⁰ A. Glenn,³⁶ A. L. Godoi,³³ Y. Goto,³² S. V. Greene,⁴⁰ M. Grosse Perdekamp,³² S. K. Gupta,² W. Guryn,³ H.-Å Gustafsson,²⁰ J. S. Haggerty,³ H. Hamagaki,⁷ A. G. Hansen,¹⁹ H. Hara,²⁴ E. P. Hartouni,¹⁸ R. Hayano,³⁸ N. Hayashi,³¹ X. He,¹⁰ T. K. Hemmick,²⁸ J. M. Heuser,²⁸ M. Hibino,⁴¹ J. C. Hill,¹³ D. S. Ho,⁴³ K. Homma,¹¹ B. Hong,¹⁵ A. Hoover,²⁶ T. Ichihara,^{31,32} K. Imai,^{17,31} M. S. Ippolitov,¹⁶ M. Ishihara,^{31,32} B. V. Jacak,^{28,32} W. Y. Jang,¹⁵ J. Jia,²⁸ B. M. Johnson,³ S. C. Johnson,^{18,28} K. S. Joo,²³ S. Kametani,⁴¹ J. H. Kang,⁴³ M. Kann,³⁰ S. S. Kapoor,² S. Kelly,⁸ B. Khachaturov,⁴² A. Khanzadeev,³⁰ J. Kikuchi,⁴¹ D. J. Kim,⁴³ H. J. Kim,⁴³ S. Y. Kim,⁴³ Y. G. Kim,⁴³ W. W. Kinnison,¹⁹ E. Kistenev,³ A. Kiyomichi,³⁹ C. Klein-Boesing,²² S. Klinksiek,²⁵ L. Kochenda,³⁰ V. Kochetkov,¹² D. Koehler,²⁵ T. Kohama,¹¹ D. Kotchetkov,⁵ A. Kozlov,⁴² P. J. Kroon,³ K. Kurita,^{31,32} M. J. Kweon,¹⁵ Y. Kwon,⁴³ G. S. Kyle,²⁶ R. Lacey,²⁷ J. G. Lajoie,¹³ J. Lauret,²⁷ A. Lebedev,^{13,16} D. M. Lee,¹⁹ M. J. Leitch,¹⁹ X. H. Li,⁵ Z. Li,^{6,31} D. J. Lim,⁴³ M. X. Liu,¹⁹ X. Liu,⁶ Z. Liu,⁶ C. F. Maguire,⁴⁰ J. Mahon,³ Y. I. Makdisi,³ V. I. Manko,¹⁶ Y. Mao,^{6,31} S. K. Mark,²¹ S. Markacs,⁸ G. Martinez,³⁴ M. D. Marx,²⁸ A. Masaike,¹⁷ F. Matathias,²⁸ T. Matsumoto,^{7,41} P. L. McGaughey,¹⁹ E. Melnikov,¹² M. Merschmeyer,²² F. Messer,²⁸ M. Messer,³ Y. Miake,³⁹ T. E. Miller,⁴⁰ A. Milov,⁴² S. Mioduszewski,^{3,36} R. E. Mischke,¹⁹ G. C. Mishra,¹⁰ J. T. Mitchell,³ A. K. Mohanty,² D. P. Morrison,³ J. M. Moss,¹⁹ F. Mühlbacher,²⁸ M. Muniruzzaman,⁵ J. Murata,³¹ S. Nagamiya,¹⁴ Y. Nagasaka,²⁴ J. L. Nagle,⁸ Y. Nakada,¹⁷ B. K. Nandi,⁵ J. Newby,³⁶ L. Nikkinen,²¹ P. Nilsson,²⁰ S. Nishimura,⁷ A. S. Nyanin,¹⁶ J. Nystrand,²⁰ E. O'Brien,³ C. A. Ogilvie,¹³ H. Ohnishi,^{3,11} I. D. Ojha,^{4,40} M. Ono,³⁹ V. Onuchin,¹² A. Oskarsson,²⁰ L. Österman,²⁰ I. Otterlund,²⁰ K. Oyama,^{7,38} L. Paffrath,^{3,*} A. P. T. Palounek,¹⁹ V. S. Pantuev,²⁸ V. Papavassiliou,²⁶ S. F. Pate,²⁶ T. Peitzmann,²² A. N. Petridis,¹³ C. Pinkenburg,^{3,27} R. P. Pisani,³ P. Pitukhin,¹² F. Plasil,²⁹ M. Pollack,^{28,36} K. Pope,³⁶ M. L. Purschke,³ I. Ravinovich,⁴² K. F. Read,^{29,36} K. Reygers,²² V. Riabov,^{30,35} Y. Riabov,³⁰ M. Rosati,¹³ A. A. Rose,⁴⁰ S. S. Ryu,⁴³ N. Saito,^{31,32} A. Sakaguchi,¹¹ T. Sakaguchi,^{7,41} H. Sako,³⁹ T. Sakuma,^{31,37} V. Samsonov,³⁰ T. C. Sangster,¹⁸ R. Santo,²² H. D. Sato,^{17,31} S. Sato,³⁹ S. Sawada,¹⁴ B. R. Schlei,¹⁹ Y. Schutz,³⁴ V. Semenov,¹² R. Seto,⁵ T. K. Shea,³ I. Shein,¹² T.-A. Shibata,^{31,37} K. Shigaki,¹⁴ T. Shiina,¹⁹ Y. H. Shin,⁴³ I. G. Sibiraki,¹⁶ D. Silvermyr,²⁰ K. S. Sim,¹⁵ J. Simon-Gillo,¹⁹ C. P. Singh,⁴ V. Singh,⁴ M. Sivertz,³ A. Soldatov,¹² R. A. Soltz,¹⁸ S. Sorensen,^{29,36} P. W. Stankus,²⁹ N. Starinsky,²¹ P. Steinberg,⁸ E. Stenlund,²⁰ A. Ster,⁴⁴ S. P. Stoll,³ M. Sugioka,^{31,37} T. Sugitate,¹¹ J. P. Sullivan,¹⁹ Y. Sumi,¹¹ Z. Sun,⁶ M. Suzuki,³⁹ E. M. Takagui,³³ A. Taketani,³¹ M. Tamai,⁴¹ K. H. Tanaka,¹⁴ Y. Tanaka,²⁴ E. Taniguchi,^{31,37} M. J. Tannenbaum,³ J. Thomas,²⁸ J. H. Thomas,¹⁸ T. L. Thomas,²⁵ W. Tian,^{6,36} J. Tojo,^{17,31} H. Torii,^{17,31} R. S. Towell,¹⁹ I. Tserruya,⁴² H. Tsuruoka,³⁹ A. A. Tsvetkov,¹⁶ S. K. Tuli,⁴ H. Tydesjö,²⁰ N. Tyurin,¹² T. Ushiroda,²⁴ H. W. van Hecke,¹⁹ C. Velissaris,²⁶ J. Velkovska,²⁸ M. Velkovsky,²⁸ A. A. Vinogradov,¹⁶ M. A. Volkov,¹⁶ A. Vorobyov,³⁰ E. Vznuzdaev,³⁰ H. Wang,⁵ Y. Watanabe,^{31,32} S. N. White,³ C. Witzig,³ F. K. Wohn,¹³ C. L. Woody,³ W. Xie,^{5,42} K. Yagi,³⁹ S. Yokkaichi,³¹ G. R. Young,²⁹ I. E. Yushmanov,¹⁶ W. A. Zajc,⁸ Z. Zhang,²⁸ and S. Zhou⁶

(PHENIX Collaboration)

¹Institute of Physics, Academia Sinica, Taipei 11529, Taiwan

²Bhabha Atomic Research Centre, Bombay 400 085 India

³Brookhaven National Laboratory, Upton, New York 11973-5000

⁴Department of Physics, Banaras Hindu University, Varanasi 221005, India

⁵University of California–Riverside, Riverside, California 92521

⁶China Institute of Atomic Energy (CIAE), Beijing, People's Republic of China

⁷Center for Nuclear Study, Graduate School of Science, University of Tokyo, 7-3-1 Hongo, Bunkyo, Tokyo 113-0033, Japan

- ⁸*Columbia University, New York, New York 10027 and Nevis Laboratories, Irvington, New York 10533*
⁹*Florida State University, Tallahassee, Florida 32306*
¹⁰*Georgia State University, Atlanta, Georgia 30303*
¹¹*Hiroshima University, Kagamiyama, Higashi-Hiroshima, 739-8526, Japan*
¹²*Institute for High Energy Physics (IHEP), Protvino, Russia*
¹³*Iowa State University, Ames, Iowa 50011*
¹⁴*KEK, High Energy Accelerator Research Organization, Tsukuba-shi, Ibaraki-ken 305-0801, Japan*
¹⁵*Korea University, Seoul, 136-701 Korea*
¹⁶*Russian Research Center "Kurchatov Institute," Moscow, Russia*
¹⁷*Kyoto University, Kyoto 606, Japan*
¹⁸*Lawrence Livermore National Laboratory, Livermore, California 94550*
¹⁹*Los Alamos National Laboratory, Los Alamos, New Mexico 87545*
²⁰*Department of Physics, Lund University, Box 118, SE-221 00 Lund, Sweden*
²¹*McGill University, Montreal, Quebec H3A 2T8, Canada*
²²*Institut für Kernphysik, University of Münster, D-48149 Münster, Germany*
²³*Myongji University, Yongin, Kyonggido 449-728, Korea*
²⁴*Nagasaki Institute of Applied Science, Nagasaki-shi, Nagasaki 851-0193 Japan*
²⁵*University of New Mexico, Albuquerque, New Mexico 87131*
²⁶*New Mexico State University, Las Cruces, New Mexico 88003*
²⁷*Chemistry Department, State University of New York–Stony Brook, Stony Brook, New York 11794*
²⁸*Department of Physics and Astronomy, State University of New York–Stony Brook, Stony Brook, New York 11794*
²⁹*Oak Ridge National Laboratory, Oak Ridge, Tennessee 37831*
³⁰*PNPI, Petersburg Nuclear Physics Institute, Gatchina, Russia*
³¹*RIKEN (The Institute of Physical and Chemical Research), Wako, Saitama 351-0198, Japan*
³²*RIKEN BNL Research Center, Brookhaven National Laboratory, Upton, New York 11973-5000*
³³*Universidade de São Paulo, Instituto de Física, Caixa Postal 66318, São Paulo CEP05315-970, Brazil*
³⁴*SUBATECH (Ecole des Mines de Nantes, IN2P3/CNRS, Université de Nantes) BP 20722-44307, Nantes-cedex 3, France*
³⁵*St. Petersburg State Technical University, St. Petersburg, Russia*
³⁶*University of Tennessee, Knoxville, Tennessee 37996*
³⁷*Department of Physics, Tokyo Institute of Technology, Tokyo, 152-8551 Japan*
³⁸*University of Tokyo, Tokyo, Japan*
³⁹*Institute of Physics, University of Tsukuba, Tsukuba, Ibaraki 305, Japan*
⁴⁰*Vanderbilt University, Nashville, Tennessee 37235*
⁴¹*Waseda University, Advanced Research Institute for Science and Engineering, 17 Kikui-cho, Shinjuku-ku, Tokyo 162-0044, Japan*
⁴²*Weizmann Institute, Rehovot 76100, Israel*
⁴³*Yonsei University, IPAP, Seoul 120-749, Korea*
⁴⁴*KFKI Research Institute for Particle and Nuclear Physics (RMKI), Budapest, Hungary[†]*
 (Received 21 March 2002; published 5 August 2002)

Data from Au + Au interactions at $\sqrt{s_{NN}} = 130$ GeV, obtained with the PHENIX detector at the Relativistic Heavy-Ion Collider, are used to investigate local net charge fluctuations among particles produced near midrapidity. According to recent suggestions, such fluctuations may carry information from the quark-gluon plasma. This analysis shows that the fluctuations are dominated by a stochastic distribution of particles, but are also sensitive to other effects, like global charge conservation and resonance decays.

DOI: 10.1103/PhysRevLett.89.082301

PACS numbers: 25.75.Dw

The PHENIX detector [1] at the Relativistic Heavy-Ion Collider (RHIC) is a versatile detector designed to study the properties of nuclear matter at extreme temperatures and energy densities, obtained in central heavy-ion collisions at ultrarelativistic energies. A central goal of these studies is to collect evidence for the existence of the quark-gluon plasma (QGP) characterized by deconfined quarks and gluons.

There are several proposed ways to experimentally verify the existence of a QGP [2]. A general problem is that many of these signals also can be produced in a hadronic

scenario, albeit special conditions of highly compressed matter have to prevail. Furthermore, it is not straightforward to determine how the various plasma signals are distorted when the deconfined matter transforms back to hadronic matter. Recent theoretical investigations [3–5] predict a drastic decrease of the event-by-event fluctuations of the net charge in local phase-space regions as a signature of the plasma state. These fluctuations are not related to the transition itself, but rather with the charge distribution in the primordial plasma state. The basic idea is that each of the charge carriers in the plasma carries less charge than

the charge carriers in ordinary hadronic matter. The charge will thus be more evenly distributed in a plasma. The main concern of the theoretical discussions is how and why the original distribution survives the transition back to ordinary matter [6,7]. Predictions, for a rapidity coverage $\Delta y \geq 1$, range up to an 80% reduction in the magnitude of the fluctuations, as measured by the variance of the net charge.

Decays of hadronic resonances influence the net charge fluctuations, whether or not deconfinement is reached. In the absence of a QGP, deviations from statistical behavior can be used to determine the abundance of, e.g., ρ and ω mesons [8]. In a hadron gas resonances are expected to decrease the fluctuations by about 25%. Globally, fluctuations will be further reduced, since charge is a conserved quantity. Although multiplicity fluctuations have been studied extensively in both hadronic and nuclear processes [9], net charge fluctuations have only recently been addressed experimentally [10,11].

In this Letter we report results from an analysis of net charge fluctuations for particles produced in Au + Au interactions at $\sqrt{s_{NN}} = 130$ GeV. The fluctuations are studied in the variables $R = n_+/n_-$, the ratio between positive and negative particles, and $Q = n_+ - n_-$, the net charge [3]. The advantages and disadvantages of these variables will also be discussed.

Information from one of the PHENIX central tracking arms (west) is used in this analysis, where events are required to have a well-defined vertex close to the center of the apparatus ($|Z| < 17$ cm), as defined by the two beam-beam counters (BBC). These cover the pseudorapidity region $3.0 < |\eta| < 3.9$. Together with the information from the two zero-degree calorimeters (ZDC), placed farther away (18 m), the BBC information is used for off-line centrality selection [12]. A total of about 5×10^5 minimum bias events has been analyzed. The PHENIX west arm spectrometer has an acceptance of 0.7 units of pseudorapidity ($-0.35 < \eta < 0.35$) and $\pi/2$ radians in azimuth φ . Charged-particle trajectories are recorded in a multiwire focusing drift chamber (DC) [13]. The combination of reconstructed DC tracks [14] with matching hits in the innermost pad-chamber plane defines the sign of the charge of the particle and also provides a high resolution measurement of the transverse momentum p_T of tracks originating from the collision vertex. Tracks with a reconstructed p_T less than 0.2 GeV/c have been excluded from the analysis due to a low reconstruction efficiency and large contributions from background sources, as revealed by simulations. No upper p_T cut has been applied.

The tracking efficiency and the charge assignment have been studied using GEANT [15] simulations. Of particular importance in this context is a realistic description of the drift chamber response, which is extracted from measured data, parametrized, and applied empirically in the simulation.

RQMD [16] simulations are used to study the detection efficiency, and the fraction of reconstructed particles that preserve their charge, as well as to evaluate the results of the analysis. The charge fluctuations in RQMD are consistent with calculations based on other hadronic models like URQMD and HIJING [3]. The overall efficiency for detecting a charged particle within the acceptance is found to be around 80% for both positive and negative particles. Correlated inefficiencies due to the limited two-track resolution and detector inhomogeneities are small enough ($< 1\%$) to be safely neglected for this analysis.

Depending on p_T , between 70% and 85% of the reconstructed tracks are in one-to-one correspondence with a primarily produced particle. The remaining tracks come from secondary interactions in the detector material and from decays, where the original charge information is lost. The composition of these tracks has been studied in detail through RQMD and GEANT. The different sources are weak decays (e.g., K_S^0 , Λ , $\bar{\Lambda}$ decays) (28%), γ conversion (16%), $\eta \rightarrow \pi^+ \pi^-$ (6%). The remaining 50% are mainly from interactions in the detector material. Instead of trying to correct the data for effects from individual sources, we have directly compared the data with the outcome of the simulations. The predictions of RQMD have been studied both with and without experimental distortions, in order to quantify the net effect. It turns out that the experimental bias pushes the value of $\nu(Q)$ closer to the stochastic limit, as will be further discussed below.

In each event the numbers of positively charged particles n_+ , negatively charged particles n_- , and their sum n_{ch} are recorded. In a stochastic scenario, with a fixed number of charged particles within the acceptance, where each particle is assigned a random charge (+1 or -1 with equal probability), the variance of the net charge, Q , is

$$V(Q) \equiv \langle Q^2 \rangle - \langle Q \rangle^2 = n_{ch}. \quad (1)$$

The normalized variance in Q is

$$\nu(Q) \equiv \frac{V(Q)}{n_{ch}} = 1. \quad (2)$$

For the charge ratio, in the stochastic scenario, $V(R) \equiv \langle R^2 \rangle - \langle R \rangle^2$ will approach the value $4/n_{ch}$ as n_{ch} increases and $\nu(R) \equiv n_{ch} \cdot V(R)$ asymptotically approaches 4. When an asymmetry between positive and negative particles is introduced, $\nu(R)$ is drastically affected, whereas the effect on $\nu(Q)$ is marginal. If we write the probability p_+ that a given particle has positive charge in the form $p_+ = \frac{1}{2}(1 + \varepsilon)$, and subsequently $p_- = \frac{1}{2}(1 - \varepsilon)$, we find $\nu(Q) = 1 - \varepsilon^2$, while the asymptotic value of $\nu(R)$ is $4 + 16\varepsilon + O(\varepsilon^2)$. Detector or reconstruction inefficiencies, which randomly remove particles independent of charge, do not influence those results in the stochastic scenario. The variance, $V(R)$, can be calculated from

$$\langle R \rangle = \frac{1}{A} \sum_{i=1}^{n_{ch}-1} \frac{n_{ch}-i}{i} \binom{n_{ch}}{i} p_+^{n_{ch}-i} p_-^i; \quad (3)$$

$$\langle R^2 \rangle = \frac{1}{A} \sum_{i=1}^{n_{ch}-1} \left(\frac{n_{ch}-i}{i} \right)^2 \binom{n_{ch}}{i} p_+^{n_{ch}-i} p_-^i,$$

where $A = 1 - p_+^{n_{ch}} - p_-^{n_{ch}}$ is the new normalization due to discarding events with n_+ or n_- equal to zero. The variance of R , even for a purely stochastic charge distribution, depends on multiplicity and on the fractions of positive and negative particles.

There are other proposed measures of net charge fluctuations. Most of these are modifications of R or Q , and deal with corrections for large charge asymmetries (i.e., $\varepsilon \neq 0$) and large acceptances. Since in our case ε is close to zero, and the fraction of observed to all produced particles in an event is small, we can safely neglect those complications [17].

The data show a small excess of positive particles, growing proportionally with n_{ch} , in qualitative agreement with calculations using RQMD and GEANT. A part of this excess comes from the intrinsic isospin asymmetry and a part from secondary interactions in the detector and surrounding material.

In Fig. 1(a), $v(R)$ and $v(Q)$ are displayed as functions of n_{ch} and $v(Q)$ is multiplied by a factor of 4 to compensate for the asymptotical difference between $v(R)$ and $v(Q)$. Both $v(Q)$ and $v(R)$ are well described by the results obtained from the stochastic scenario.

Since $v(Q)$ is independent of n_{ch} one expects $v(Q)$ to be close to unity also in representations where other centrality measures are used. On the other hand, since $v(R)$ depends on multiplicity, it will have a complicated behavior as a function of centrality, making it difficult to draw any further conclusions. We will thus focus on $v(Q)$ for the rest of this analysis.

In Fig. 1(b), $v(Q)$ is displayed as a function of centrality based on the ZDC/BBC information. The full event sample, corresponding to 92% of the inelastic cross section [12], is divided into 20 centrality classes, where each class corresponds to 5% of the events. Class 20 represents the most central events. With the increased resolution on the y axis in Fig. 1(b), it is evident that $v(Q)$ is consistently below unity and deviates from stochastic behavior. The value is, however, far above the most optimistic QGP predictions $v(Q) \sim 0.2$ [3], although one should keep in mind that our coverage in rapidity is at the limit for these predictions and that we have only partial coverage in azimuth.

There may be other explanations for deviations from stochastic behavior than the one offered by the quark-gluon plasma. These include global charge conservation and neutral resonances decaying into correlated pairs of one positive and one negative particle. Both of these effects will decrease the fluctuations, and the decrease will grow in

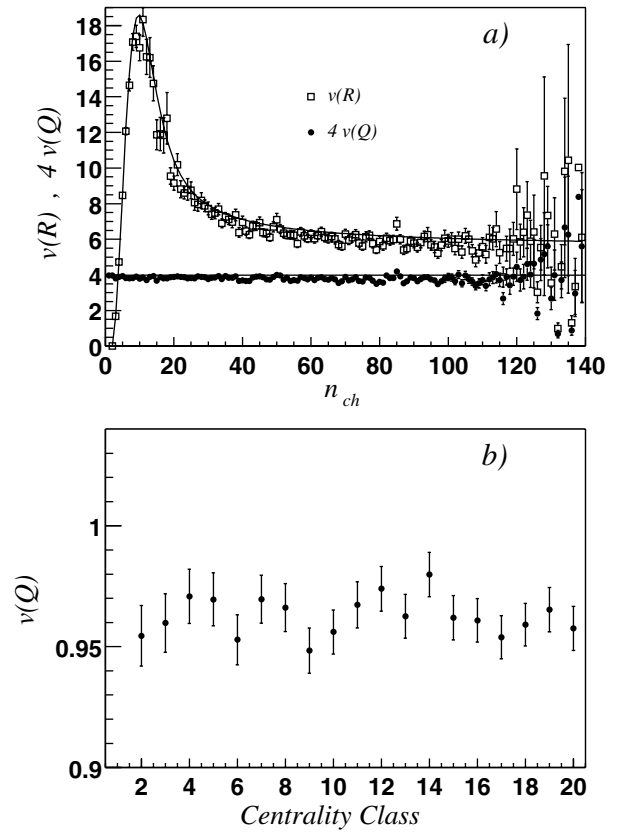


FIG. 1. (a) The normalized variances $v(Q)$ and $v(R)$ as functions of n_{ch} , together with curves for stochastic behavior. (b) The normalized variance $v(Q)$ for different centrality classes, as described in the text.

proportion to the experimental acceptance. In a stochastic scenario, taking global charge conservation into account, the normalized variance $v(Q)$ becomes $(1 - p)$, where p is the fraction of observed charged particles among all charged particles in the event. Eventually, if all charged particles are detected, $v(Q)$ will become 0.

Experimentally we can change the fraction p of particles within the acceptance by using different regions of the PHENIX west arm. In Fig. 2(a), $v(Q)$, for the 10% most central events, is displayed as a function of $\Delta\varphi_d$, i.e., the chosen azimuthal interval of the spectrometer. For comparison, the results from RQMD processed through GEANT are shown. The data and the simulation show a similar trend. Note that the data points are correlated since the data in one bin is a subset of the data in the next. The error band indicates the total statistical error in each data point. The error bars represent the uncorrelated part of this statistical error. For RQMD, only the total statistical error is given. The solid line corresponds to the $(1 - p)$ dependence discussed above. The linear relationship between p and $\Delta\varphi_d$ is estimated from the phase-space distribution of particles in RQMD, including effects from reconstruction efficiency and background tracks. For larger angles, both data and the RQMD results lie consistently below the line,

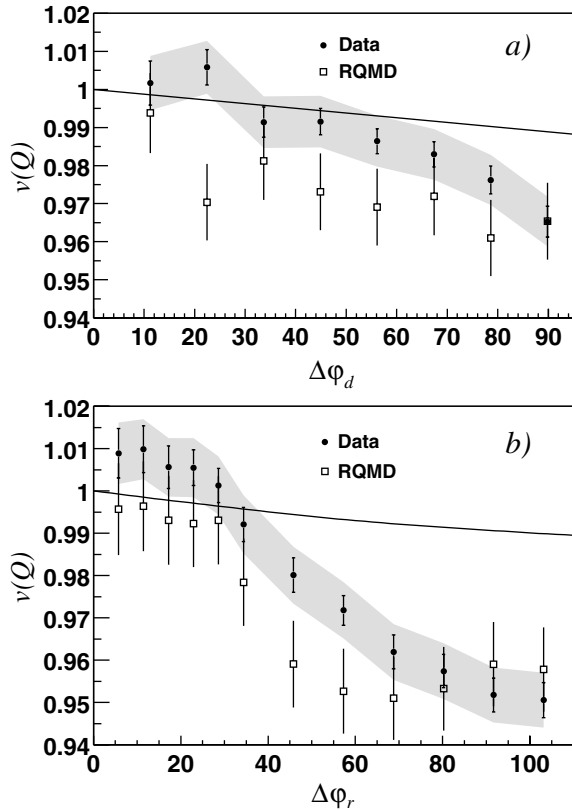


FIG. 2. $\nu(Q)$ for the 10% most central events in data and RQMD, as a function of the azimuthal coverage. For data, the error band shows the total statistical error, whereas the error bars indicate the uncorrelated part. The solid line (curve) shows the expected reduction in $\nu(Q)$ in the stochastic scenario when global charge conservation is taken into account. Azimuthal angle (in degrees) defined (a) as detector coverage, and (b) as reconstructed at the interaction vertex.

which indicates that effects from resonance decays are important.

Because of the influence of the magnetic field the positive and negative particles will have different azimuthal acceptance. On the average a charged particle (surviving the experimental cuts) will be deflected 19° in the magnetic field. The $\Delta\varphi_d$ study in Fig. 2(a) thus selects partly nonoverlapping regions of phase space for positive and negative particles. A remedy for this is to use the reconstructed φ angle for each particle φ_r , i.e., the azimuthal direction of the particle at the primary vertex, before it is deflected by the magnetic field. By choosing the azimuthal interval $\Delta\varphi_r$ symmetrically around the center of the acceptance, a better phase-space overlap is achieved for small azimuthal intervals. In Fig. 2(b), $\nu(Q)$, for the 10% most central events, is displayed as a function of $\Delta\varphi_r$. The $(1-p)$ dependence, which is no longer linear, is given by the solid curve. Again data and the RQMD results show a similar trend, but the deviations from the curve are larger in this representation, indicating that an overlap in

phase space is of importance. The errors are treated as in Fig. 2(a).

The effects of the detector inefficiency and background tracks not assigned the correct charge have been investigated in a Monte Carlo simulation. The reconstruction efficiency and the amount of background have been determined from the RQMD and GEANT simulations discussed earlier. Both the inefficiency and the background contribution have the net effect of diluting the signal and pushing the value of $\nu(Q)$ closer to 1. The dilution due to these effects can be treated as an experimental systematic error, estimated from the simulations, setting a lower limit on $\nu(Q)$. For the net charge fluctuations in the region $-0.35 < \eta < 0.35$, $p_T > 0.2$ GeV/c, and $\Delta\varphi = \pi/2$,

$$\nu(Q) = 0.965 \pm 0.007(\text{stat}) - 0.019(\text{syst}) \quad (4)$$

is obtained for the 10% most central events. Assuming a linear behavior, an extrapolation of this value to full azimuthal coverage gives a value of $\nu(Q)$ in the range 0.78–0.86, in qualitative agreement with calculations from a hadronic gas.

Our findings are in agreement with the preliminary conclusions of NA49 [10] and STAR [11] that no indication of decreased fluctuations due to quark-gluon plasma formation is observed. STAR also attributes the deviations from a stochastic scenario to be consistent with resonance correlations.

To summarize, we have shown that the data behave in an almost stochastic manner. There are also clear indications that effects from hadronic decays are seen; the data are in good agreement with RQMD calculations, which includes the effects of global charge conservations as well as neutral hadronic resonance decays. Furthermore, the data show no centrality dependence, which is in contradiction with the expectations from a quark-gluon plasma scenario. We have clearly demonstrated that the fluctuations of the charge ratio $\nu(R)$ and of the net charge $\nu(Q)$ are well understood in a stochastic model. The R variable [3] unnecessarily complicates the evaluation of the fluctuations, and the intrinsic decrease of $\nu(R)$, as a function of centrality, can be mistaken for a “plasma fingerprint.”

The measured value of $\nu(Q) = 0.965$ is far from the value predicted for a plasma. Even extrapolating the linear trend seen in the data in Fig. 2(a) to full azimuthal coverage renders values of the fluctuations, which are far above the proposed values. With the caveat of our limited acceptance in rapidity, these results clearly indicate either the absence of a plasma or a proposed signal that does not survive the transition back to hadronic matter.

We thank the staff of the Collider-Accelerator and Physics Departments at BNL for their vital contributions. We acknowledge support from the Department of Energy and NSF (U.S.A.), MEXT and JSPS (Japan), RAS, RMAE, and RMS (Russia), BMBF, DAAD, and AvH (Germany), VR and KAW (Sweden), MIST and NSERC (Canada),

CNPq and FAPESP (Brazil), IN2P3/CNRS (France), DAE and DST (India), KRF and CHEP (Korea), the U.S. CRDF for the FSU, and the U.S.-Israel BSF.

*Deceased.

†Not a participating Institution.

- [1] PHENIX Collaboration, D.P. Morrison *et al.*, Nucl. Phys. **A638**, 565c (1998).
- [2] For example, J.-P. Blaizot, Nucl. Phys. **A661**, 3c (1999).
- [3] S. Jeon and V. Koch, Phys. Rev. Lett. **85**, 2076 (2000); M. Bleicher, S. Jeon, and V. Koch, Phys. Rev. C **62**, 061902(R) (2000).
- [4] M. Asakawa, U. Heinz, and B. Müller, Phys. Rev. Lett. **85**, 2072 (2000).
- [5] H. Heiselberg and A.D. Jackson, Phys. Rev. C **63**, 064904 (2001).
- [6] E.V. Shuryak and M.A. Stephanov, Phys. Rev. C **63**, 064903 (2001).
- [7] K. Fialkowski and R. Wit, Europhys. Lett. **55**, 184 (2001).
- [8] S. Jeon and V. Koch, Phys. Rev. Lett. **83**, 5435 (1999).
- [9] For example, E. A. De Wolf, I.M. Dremin, and W. Kittel, Phys. Rep. **270**, 1 (1996).
- [10] NA49 Collaboration, S.V. Afanasiev *et al.*, Nucl. Phys. **A698**, 104c (2002).
- [11] STAR Collaboration, J.G. Reid *et al.*, Nucl. Phys. **A698**, 611c (2002).
- [12] PHENIX Collaboration, K. Adcox *et al.*, Phys. Rev. Lett. **86**, 3500 (2001).
- [13] V.G. Riabov, Nucl. Instrum. Methods Phys. Res., Sect. A **419**, 363 (1998).
- [14] J.T. Mitchell *et al.*, Nucl. Instrum. Methods Phys. Res., Sect. A **482**, 491 (2002).
- [15] GEANT 3.21, CERN program library, 1993.
- [16] H. Sorge, Phys. Rev. C **52**, 3291 (1995).
- [17] S. Mrowczynski, nucl-th/0112007 (to be published); private communication.